
NESTQUANT: NESTED LATTICE QUANTIZATION FOR MATRIX PRODUCTS AND LLMs

Semyon Savkin*
MIT
semyon@mit.edu

Eitan Porat*
Independent
ethan.porat@gmail.com

Or Ordentlich
Hebrew University of Jerusalem
or.ordentlich@mail.huji.ac.il

Yury Polyanskiy
MIT
yp@mit.edu

ABSTRACT

Post-training quantization (PTQ) has emerged as a critical technique for efficient deployment of large language models (LLMs). This work proposes NESTQUANT, a novel PTQ scheme for weights and activations that is based on self-similar nested lattices. Recent work have mathematically shown such quantizers to be information-theoretically optimal for low-precision matrix multiplication. We implement a practical low-complexity version of NestQuant based on Gosset lattice, making it a drop-in quantizer for any matrix multiplication step (e.g., in self-attention, MLP etc). For example, NestQuant quantizes weights, KV-cache, and activations of Llama-3-8B to 4 bits, achieving perplexity of 6.6 on wikitext2. This represents more than 55% reduction in perplexity gap with respect to unquantized model (perplexity of 6.14) compared to state-of-the-art Meta’s SpinQuant (perplexity 7.3). Comparisons on various LLM evaluation benchmarks also show a reduction in performance degradation induced by quantization.

1 Introduction

There are three principal goals of post-training quantization (PTQ). First, reducing the number of bits per parameter allows for loading big models on cheap GPUs with limited memory, thus democratizing access to LLMs. This requires “weights-only” quantization algorithms of which the most popular are AWQ, GPTQ, and QuIP (see references in Section 2.2).

The second goal of PTQ is to accelerate inference. In LLMs most of the compute is spent multiplying matrices. Multiplying a pair of such matrices requires $2n^3$ FLOPs and $\frac{3}{8}Rn^2$ bytes to exchange between the core and memory (here and below R designates the number of bits required to store each entry of a vector/matrix). So when matrices are large (such as during the pre-fill phase when the prompt is processed) the GPU is compute-bound, while when n is small (such as during generation) the GPU becomes memory-bound. To achieve this goal one needs to reduce R by quantizing both weights and the KV cache.

The third goal of PTQ is to accelerate inference of giant LLMs that require hosting each layer on a separate GPU (pipelining parallelism). For this goal one needs to quantize activations passed from one layer to the next to reduce the communication bottleneck.

While quantization of weights to $R = 3, 4$ and even $R = 2$ bits has been achieved with minimal loss of quality, quantiza-

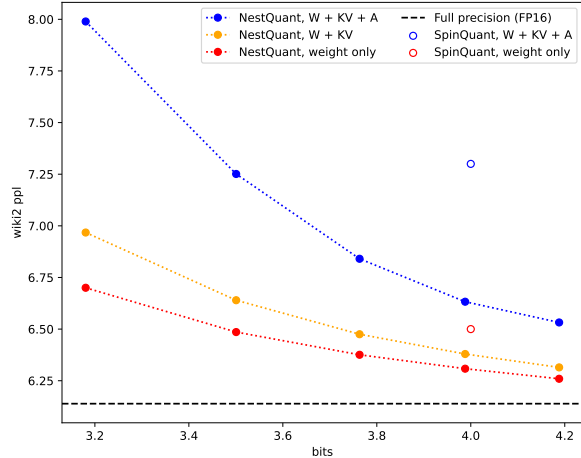


Figure 1: Perplexity of quantized models for three regimes (weight-only, weights + KV cache, end-to-end) on wikitext2 vs number of bits per entry.

*Equal contribution

tion of KV cache and activations has been much more challenging. Popular algorithms for full quantization are LLM.int8(), SmoothQuant and SpinQuant (see references in Section 2.2), the latter having state-of-the-art performance. This work proposes an alternative algorithm (NestQuant) for quantizing weights, KV-cache, and activations. The algorithm is motivated by recent theoretical work on approximate matrix multiplication and follows several classical ideas such as the Conway-Sloane algorithm for the Gosset lattice.

1.1 Summary of results

Model	Bits ↓	Bits (no zstd) ↓	ARC-C ↑	ARC-E ↑	Hellaswag ↑	PIQA ↑	Winogrande ↑	Zero-shot Avg ↑	Wikitext2 ppl ↓
Baseline (FP16)	16	16	0.54	0.78	0.79	0.81	0.74	0.73	6.1
Weights only									
LLM-QAT	4.00	-	0.51	0.77	0.48	0.79	0.72	0.65	7.7
GPTQ	4.00	-	0.47	0.72	0.74	0.77	0.71	0.68	7.2
SpinQuant	4.00	-	0.54	0.77	0.78	0.80	0.72	0.72	6.5
NestQuant $q = 14, k = 4$ (ours)	3.99	4.06	0.53	0.78	0.79	0.80	0.73	0.72	6.3
Weights + KV cache									
SpinQuant	4.00	-	0.51	0.77	0.77	0.78	0.69	0.70	6.6
NestQuant $q = 14, k = 4$ (ours)	3.99	4.06	0.53	0.78	0.79	0.79	0.74	0.72	6.4
Weights, KV cache, activations									
LLM-QAT	4.00	-	0.27	0.41	0.38	0.60	0.53	0.44	52.5
Quarot	4.00	-	0.44	0.67	0.75	0.75	0.66	0.67	8.4
SpinQuant	4.00	-	0.51	0.75	0.75	0.77	0.66	0.68	7.3
NestQuant $q = 14, k = 4$ (ours)	3.99	4.06	0.51	0.75	0.78	0.79	0.72	0.71	6.6

Table 1: 4-bit quantization of Llama-3-8B. The bits column for NestQuant corresponds to actually measured average number of bits per entry (when a vector of auxiliary scaling coefficients β is compressed via zstd) and the second column shows quantization rate when no compression step is used.

The NestQuant algorithm is described in Section 4. NestQuant is a generic drop-in replacement for any matrix multiplication. Its performance for synthetic random Gaussian matrices comes pretty close to information-theoretic limits (see Fig. 3) and significantly outperforms uniform quantization employed by SpinQuant. Switching from a scalar (uniform) quantization to vector quantization requires some price to pay computationally (Section C), however, among vector quantizers NestQuant is rather economical as it operates in dimension 8 and leverages an elegant algorithm of [1].

Applying NestQuant to quantizing an actual LLM (Llama-3-8B) shows massive end-to-end improvement: Fig. 1 shows a significant reduction of perplexity compared to SpinQuant; and Table 1 confirms enhanced performance on standard LLM benchmarks.

The main source of improvement of NestQuant is demonstrated in Fig. 2 (although NestQuant uses an 8-dimensional Gosset lattice, not a 2D hexagonal one). More details on this as well as directions for improvement are discussed in Section 3.

Thus, we believe that NestQuant offers an excellent alternative to other algorithms. It quantizes weights, KV-cache and activations, achieves significant improvement on both synthetic and real data.

1.2 Paper organization

We start with a detailed review of classical work on vector quantization and modern LLM quantization (Section 2). Then in Section 3 we explain the motivation for each step of the algorithm. Section 4 contains the pseudocode of the algorithm and diagram of quantized LLM. Finally, Section 5 concludes with details about empirical performance. Further details and evaluations are relegated to the Appendices.

2 Prior work

We briefly survey prior work, which we separate into work by information theorists and by the ML community.

2.1 Information-theoretic quantization

Rate R quantization of an information source X in \mathbb{R}^n is the operation of encoding it to nR bits, from which a decoder can produce a reconstruction $\hat{X} \in \mathbb{R}^n$ that has small *distortion* with respect to X . The most popular distortion criterion is the quadratic loss, where the expected distortion is defined as $D = \frac{1}{n} \mathbb{E} \|X - \hat{X}\|^2$, and here we restrict attention to this loss. Characterization of the optimal tradeoff between R and D is a classic topic in information theory, e.g. [2, Part V].

For a Gaussian source $X \sim \mathcal{N}(0, I_n)$ the rate-distortion theorem states that any compressor at rate R must satisfy $D \geq D(R) \triangleq 2^{-2R}$. Furthermore, as dimension n increases there exist quantizers with distortion approaching $D(R)$. Notably, such quantizers can be made universal, in the sense that they attain distortion $D(R)$ not only for iid Gaussian X but for any (even adversarial) input as long as its Euclidean norm is $(1 + o(1))\sqrt{n}$.

One way for constructing these universal quantizers is based on lattices [3] that admit much more structure than more classical random codes (and ϵ -nets).

Arguably, the most notable lattice-based quantization scheme is the family of Voronoi codes [1], which we use in this work.

How does one convert a quantizer adapted to Gaussian inputs to work (with the same guaranteed loss) on non-Gaussian data? In a nutshell, the idea is simple: if U is chosen to be a random $n \times n$ orthogonal matrix then the entries of UX will be distributed as iid Gaussian [4]. This idea of applying random rotations to smooth out the distribution of the quantizer’s input may be viewed as a special case of high-dimensional companding [5], and has been applied for image compression [6], and as a potential replacement for dithering [7], to name a few.

In the context of LLMs, the goal in quantization is slightly different since quantization is used to facilitate approximate matrix multiplication with reduced burden on the memory bandwidth. For example, when quantizing two vectors $X, Y \in \mathbb{R}^n$ the goal is *not* to approximate them but to approximate their inner product. Recently, information-theoretic characterization of this task was completed in [8]. Specifically, the authors show that if $X, Y \sim \mathcal{N}(0, I_n)$ are independent then for any algorithm operating on the basis of rate- R quantized representations of X and Y we must have

$$\mathbb{E}(X^\top Y - \widehat{X^\top Y})^2 \geq n\Gamma(R), \tag{1}$$

where

$$\Gamma(R) = \begin{cases} 1 - (1 - (2 \cdot 2^{-2R^*} - 2^{-4R^*})) \frac{R}{R^*} & R < R^* \\ 2 \cdot 2^{-2R} - 2^{-4R} & R \geq R^* \end{cases} \tag{2}$$

and $R^* \approx 0.906$ is a solution to a certain transcendental fixed-point equation.

The same paper also constructs *universal quantizers* based on nested lattices that asymptotically (as $n \rightarrow \infty$) achieve this lower bound. Note that extension from vectors to matrices can be made trivially by observing that one can quantize each column separately and treat matrix product as a collection of inner products.

In this work we show that with appropriate tweaks Voronoi codes indeed can result in practical fast and efficient algorithms for LLM quantization. We emphasize that most of our work is on simply developing a drop-in replacement for quantized matrix product and as such is not specific to LLMs.

The idea of applying random rotations to “Gaussianize” inputs in the context of approximate inner product computation is even more natural than in the standard quantization. Indeed, since one is only interested in the inner product, not vectors themselves, one does not need to store (even a seed used to generate the) random orthogonal matrix. This has been long exploited in locality-sensitive hashing (LSH) algorithms,* which can be viewed as an (extremely low rate) quantizers for inner product approximation [9, 10, 11]. Unsurprisingly, as we will see next, random rotations have also been found quite useful for quantizing LLMs.

2.2 LLM quantization

One of the directions of prior research on LLM quantization is addressing the issue of activation outliers that hinder the quantization quality. These outliers are present in certain dimensions of activations, weights and KV cache. In LLM.int8() of [12], these outlier dimension are kept unquantized. In SmoothQuant [13] authors balance the scale of outliers between weights and activations by modifying LayerNorm’s diagonal matrices.

Going to random rotations, by rewriting matrix product $AB = (AU)(U^\top B)$ for an orthogonal matrix U , one gets matrices with much more Gaussian entries (few outliers) and can apply standard quantization algorithms. Some of the multiplications by U can be merged with the weights (i.e. do not require additional runtime FLOPs), while the rest are applied at runtime. For the latter, matrices U should have structure to enable fast multiplication. For example, QuaRot [14] uses randomized Hadamard matrices as coordinate transformations, which can be applied to a vector of size n in $O(n \log n)$ additions. SpinQuant [15] uses a rotation parametrization with four orthogonal matrices R_1, R_2, R_3, R_4 , where R_1 and R_2 can be arbitrary orthonormal matrices, and R_3 and R_4 should have a fast multiplication algorithm. The authors use Cayley SGD [16] to optimize R_1 and R_2 for minimization of the quantization error, while the matrices R_3 and R_4 are chosen to be random Hadamard.

*In LSH, one typically performs several random *projections* of the vector and quantizes them. This is equivalent to performing random rotation and quantizing only a small number of entries of the rotated vector.

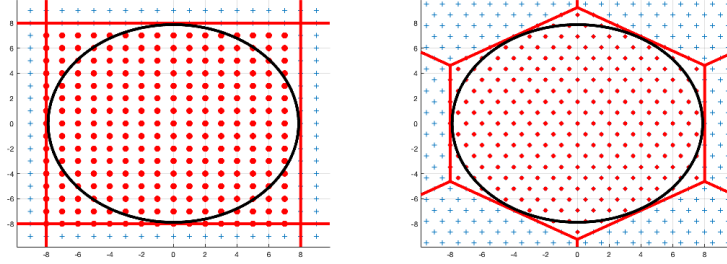


Figure 2: Demonstrating advantage of NestQuant in 2D. Typical weights and activations are vectors inside the black circle. Uniform quantization wastes about 32% of allocated bitstrings for vectors outside of the circle, while nested hexagonal lattices only wastes 15% (explicitly enumerating points inside the circle to avoid the waste is too slow to do at runtime). This allows NestQuant to use finer grid while quantizing to the same rate R . The gain becomes much more dramatic in higher dimensions.

Starting from `LLM.int8()` most of the schemes used uniform quantization (i.e. where a floating point vector simply rounded to a nearest integer after an appropriate rescaling). To the best of our knowledge, so far non-scalar quantization has only been used for weight-only compression for LLMs in QuIP# [17], which uses E8P codebook for 2-bit quantization, and applies Residual Vector Quantization [18] to get a 4-bit quantization scheme; and QTIP [19] which uses trellis codebook. Unfortunately these methods appear to be too expensive to apply then in runtime, perhaps explaining why non-uniform quantization for activations and KV-cache was not attempted before this work.

Finally, when quantizing weight matrices, one may notice that MSE distortion loss should be replaced by a weighted-MSE loss dependent on the statistics of the incoming activations. We refer to this type of algorithms as LDLQ, following authors of QuIP [20], QuIP# [17] and GPTQ [21]. Applying LDLQ-modified NestQuant does lead to improved performance, see results in Section 5.

3 Outline of NestQuant approach

In this section we outline the main components of our approach. A detailed description is brought in the following section.

When designing a quantizer, one needs to make some assumptions about the distribution of the source that will be fed to it. While weights (and sometimes activations) can be well-approximated by Gaussians, their magnitude are wildly varied. Thus, one employs two ideas: normalization and random rotation.

Normalization: In most of the literature, the normalization is done by taking an input vector of large dimension n (e.g. $n = 4096$ for Llama-3), dividing by the L_∞ norm to get entries to be in $[-1, 1]$ and then applying uniform quantization. This is suboptimal for two reasons: one is that uniform quantization induces error that is distributed uniformly on the small cube, which is suboptimal from the MSE point of view. Second reason, much more serious, is known as the shaping gain and demonstrated on Fig. 2. When entries of the vector are Gaussian, it will typically lie inside the black circle. Thus those grid elements outside of it will almost never be used, wasting bitspace.

Instead, we use normalization by the L_2 -norm (see Algorithm 3) and then use points inside the Voronoi region of a Gosset lattice, which as Fig. 2 (right) demonstrates wastes a lot fewer bitstrings for rare vectors, thus allowing us to use finer grids.

Random rotation: When input to the quantizer significantly differs from the presumed model (of iid Gaussians), performance can become quite poor. As discussed previously, multiplying by a random orthogonal matrix U provides an excellent fix. Specifically, UX vector becomes uniform on the n -sphere of radius \sqrt{n} , and small chunks of this vector have distribution very close to Gaussian iid. In particular, the total variation between any subset of d coordinates and $\mathcal{N}(0, I_d)$ is $O(d^2/n)$ [4], such that for $d = o(\sqrt{n})$ what we quantize is effectively iid Gaussian.

Complexity of lattice quantization: In order to explain our choice of nested lattice quantizer, we need to carefully balance several requirements. One of the key ones is complexity. It is known that finding (even approximating) a nearest lattice point is a well-known cryptographic assumption [22]. Thus, we are not suggesting to directly operate on n -dimensional lattices. Instead, we partition the n -vector into sections, each of dimension d and apply lattice quantization to d -subvectors. Equivalently, our vector quantizers for \mathbb{R}^n are constructed as Cartesian products of vector quantizers of small dimension d (we will take $d = 8$ for all experiments).

Granular and overload quantization errors: There are two different sources of errors for lattice quantizers. The first is called *granular* quantization error, and is related to the second moment of the lattice Voronoi region. A common way to measure the

granular error corresponding to a lattice $\Lambda \subset \mathbb{R}^d$ is via the normalized second moment (NSM) defined as

$$G(\Lambda) = \frac{1}{\text{vol}(\mathcal{V}_\Lambda)^{1+\frac{2}{d}}} \frac{1}{d} \int_{x \in \mathcal{V}_\Lambda} \|x\|^2 dx, \quad (3)$$

where $\mathcal{V}_\Lambda \subset \mathbb{R}^d$ is the Voronoi region of Λ , consisting of all point in \mathbb{R}^d closer to 0 than to any other lattice point in Λ . This quantity corresponds to the MSE when Λ is normalized to have unit covolume and is then used as a quantizer. It is well known that the optimal (smallest) NSM among all lattices in \mathbb{R}^d approaches $\frac{1}{2\pi e}$ from above as d increases [3]. Furthermore, for $d = 1$ we get $G(\mathbb{Z}) = \frac{1}{12}$. Consequently, in terms of granular error, by using high-dimensional lattices instead of the simple scalar quantizer based on \mathbb{Z} we can already gain a factor of $\frac{2\pi e}{12} \approx 1.42329$ in performance (the Gosset lattice achieves 1.22 gain).

Notice, however, that representing x as $Q_\Lambda(x)$, the nearest lattice point in Λ , requires infinitely many bits, since the lattice is infinite. Since we only have 2^{dR} bitstrings to allocate, we need to select a subset of Λ that will be actually used. Selection of \mathcal{S} so that $|\Lambda \cap \mathcal{S}| = 2^{dR}$ is called *shaping*. If $Q_\Lambda(x) \in \mathcal{S}$, then the quantization error $x - Q_\Lambda(x)$ will be in \mathcal{V}_Λ and we will only suffer from a granular error. However, when $Q_\Lambda(x) \notin \mathcal{S}$ the quantization error is no longer in \mathcal{V}_Λ and may be have much greater magnitude than a typical granular error. We refer to those type of errors, where $Q_\Lambda(x) \notin \mathcal{S}$, as *overload* errors.

Generally speaking, in order to achieve a small quantization error, one must keep the probability of overload very small. This can be attained by scaling up the codebook to $\beta\mathcal{C} = \beta\Lambda \cap \beta\mathcal{S}$ with a large enough $\beta > 0$ such that overload becomes very rare. However, increasing β also increases the squared granular error by a factor of β^2 . Thus, one would like to use the smallest possible β for which overload is rare. In order to allow for smaller β , we would like to choose $\mathcal{S} \subset \mathbb{R}^n$ such that $\beta\mathcal{S}$ captures as much Gaussian mass as possible.

Denote by $\mu = \mathcal{N}(0, I_d)$ the standard Gaussian measure. Since we need $2^{dR} = |\Lambda \cap \mathcal{S}| \approx \frac{\text{vol}(\mathcal{S})}{\text{covol}(\Lambda)}$, a good shaping region \mathcal{S} maximizes $\mu(\mathcal{S})$, which in turn minimizes the overload probability that is approximated by $1 - \mu(\mathcal{S})$, under a volume constraint. Clearly, the optimal \mathcal{S} under this criterion is $r\mathcal{B}$ where $\mathcal{B} = \{x \in \mathbb{R}^d : \|x\| \leq r_{\text{eff}}(1)\}$ is a Euclidean ball with radius $r_{\text{eff}}(1)$ chosen such that $\text{vol}(\mathcal{B}) = 1$, and r is chosen such that $\text{vol}(\mathcal{S}) = r^d$ satisfies the required volume constraint. Unfortunately, for $d > 1$ the codebook $\mathcal{C} = \Lambda \cap r\mathcal{B}$ loses much of the lattice structure, and does not admit an efficient enumeration, and consequently encoding and decoding require using a lookup table (LUT). QuIP# used this approach with $\Lambda = E_8$ (same as we do) and $\mathcal{S} = r\mathcal{B}$. However, this seems to only be possible for quantizing weights and not activations as complexity makes runtime implementation too slow.[†]

Using int8-multipliers: One often mentioned advantage of uniform quantization compared to other approaches is the fact that it approximates any matrix as a product of diagonal matrix (of norms) and an integer matrix. Thus, during multiplication one can leverage faster int-cores rather than floating-point multiplication. Note that if there exists a scaling coefficient $\alpha > 0$ such that $\alpha\Lambda \subset \mathbb{Z}^d$, then one can still use int-multipliers even for lattice-quantized vectors.

Voronoi codes/nested lattice codes: In Voronoi codes [1] the same lattice Λ is used for both quantization and shaping. In particular, the shaping region is taken as $\mathcal{S} = 2^R\mathcal{V}_\Lambda$, where 2^R is an integer. As elaborated below, if $Q_\Lambda(x)$ admits an efficient implementation, one can efficiently perform encoding and decoding to the codebook $\mathcal{C} = \Lambda \cap (2^R\mathcal{V}_\Lambda) \cong \Lambda/2^R\Lambda$. Moreover, in stark contrast to ball-based shaping, the encoding and decoding complexity does not depend on R .

In summary, a good choice of lattice Λ should therefore have: 1) efficient lattice decoding algorithm; 2) small NSM; 3) large $\mu(\mathcal{V}_\Lambda)$; 4) be a subset of standard integer lattice \mathbb{Z}^d .

In this work, we use the Gosset lattice (E_8) that satisfies all these properties. It has a fast decoding algorithm (Algorithm 5), its NSM is $\approx 0.0716821 \approx 1.2243 \frac{1}{2\pi e}$ [23], and its Gaussian mass $\mu(r\mathcal{V}_{E_8})$ is very close to $\mu(r\mathcal{B})$ (the Gosset lattice has unit covolume, so $\text{vol}(r\mathcal{V}_{E_8}) = \text{vol}(r\mathcal{B})$). The last point is illustrated in Figure 6, where the large loss for cubic shaping with respect to lattice shaping is also evident. The gap between Voronoi/Ball shaping and cubic shaping becomes much more significant as the dimension increases. This follows since for large d we have that for $X \sim \mu = \mu_d$ the ℓ_∞ norm $\|X\|_\infty$ concentrates around $\sqrt{2 \ln d}$. Thus, for $r < 2\sqrt{2 \ln d}$ we have that $\mu(r\text{CUBE}) \rightarrow 0$, whereas for any $r > \frac{\sqrt{d}}{r_{\text{eff}}(1)} = \sqrt{2\pi e}(1 + o(1))$ we have that $\mu(r\mathcal{B}) \rightarrow 1$. Note that SpinQuant uses high-dimensional cubic shaping, and therefore its MSE distortion suffers a $O(\ln d)$ multiplicative gap with respect to the optimal distortion.

Overload avoidance via union of Voronoi codes: Because we rely on lattice quantizers of relatively small dimension ($d = 8$), even if $\mu(r\mathcal{V}_\Lambda)$ is very close to $\mu(r\mathcal{B})$, overload events are unavoidable. This follows because in small dimension the norm of a iid Gaussian vector is not sufficiently concentrated. Thus, if one is restricted to $\mathcal{C} = \beta(\Lambda \cap (2^R\mathcal{V}_\Lambda))$ the parameter β must be taken quite large in order to keep the overload probability small. This in turn, incurs a significant penalty in the obtained distortion. As a remedy, rather than using a Voronoi code, we take \mathcal{C} as a union of (a small number) of Voronoi codes in different

[†]We note that QuIP# cleverly exploits symmetries of E_8 to show that an $R = 2$ bit quantizer can be implemented using an LUT of size $2^{d\frac{R}{2}} = 2^8$, but we believe this is still too slow, and furthermore does not naturally extend to different quantization rates.

scales. Namely, we take $\mathcal{C} = \cup_{t=1}^k \beta_t (\Lambda \cap (2^R \mathcal{V}_\Lambda))$, where $\beta_1 < \dots < \beta_k$. The smallest values of β_t are set such that overload is not too common but not extremely rare, such that for most realizations of a Gaussian vector $X \in \mathbb{R}^d$ the distortion is close to the fundamental limit $D(R)$. Whenever X is atypically large, there will be overload in $\beta_t (\Lambda \cap (2^R \mathcal{V}_\Lambda))$ for small t , but not for large t , such that the quantization error will be in $\beta_t \mathcal{V}_\Lambda$ for one of the larger values of $\{\beta_t\}$.

The details of choosing k and values of β_t are described in Section D. Here we only note that the overall compression rate becomes $R + \frac{1}{d} \log_2 k$. In some cases, we are using nvcomp [24] for compressing a vector of $n/8$ chosen betas, in which case rate penalty is reduced below $\frac{1}{d} \log_2 k$. We note that in our comparisons, including Table 1, we always use this effective rate for a fair comparison with other algorithms.

NestQuant, SpinQuant and theory: As mentioned above, the use of nested lattice codes is rooted in theory. In [8] it was shown that nested lattice quantizers of high-dimensions attain the optimal rate-distortion tradeoff for matrix multiplication. Since the lattices used for proving that result do not admit efficient lattice decoding, here we resort to n -dimensional lattices constructed as the Cartesian product of $n/8$ copies of the Gosset lattice, whose dimension is $d = 8$. To understand how much loss in efficiency this leads, Fig. 3 compares NestQuant, SpinQuant (uniform quantization with cubic shaping) and information-theoretic lower bound (1). Details of this experiment can be found in Section 5.1. We can see that NestQuant is reasonably close to the fundamental limit and significantly outperforms SpinQuant.

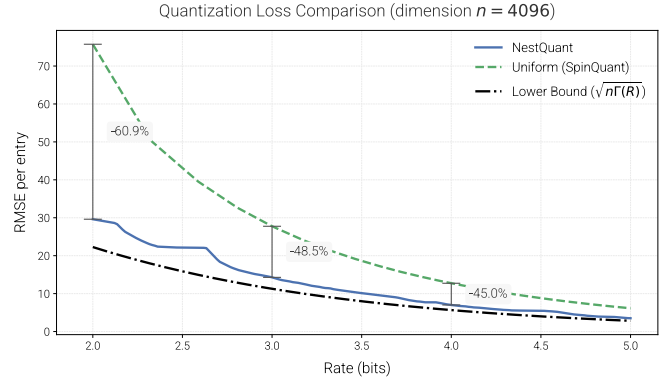


Figure 3: RMSE for quantized matrix multiplication for iid $\mathcal{N}(0, 1)$ matrices. NestQuant algo is optimized over q and multiple β 's. Also shown is information-theoretic lower bound from (1).

4 Detailed Method

4.1 Nested lattice codebook

In this section, we describe the construction for a Vector Quantization (VQ) codebook of size q^d for quantizing an d -dimensional vector, where q is an integer parameter. To quantize a vector, we find the closest codebook element by Euclidean norm. We describe efficient encoding and decoding algorithms to a quantized representation in \mathbb{Z}_q^d .

Let Λ be a lattice in \mathbb{R}^d with generator matrix G . We define the coordinates of a point $x \in \Lambda$ to be an integer vector v such that $x = Gv$. Each point $P \in \Lambda$ has a corresponding Voronoi region $\mathcal{V}_\Lambda(P)$, for which P is the closest point in Λ with respect to L^2 metric. To define the codebook, we consider the scaled lattice $q\Lambda$. Then:

Definition 4.1. $x \in \Lambda$ belongs to codebook C iff $x \in \mathcal{V}_{q\Lambda}(0)$. Let v be the coordinates of x . Then, the quantized representation of x is $\mathcal{Q}(x) := v \bmod q$. Note that \mathcal{Q} is a bijection between C and \mathbb{Z}_q^d

Using this representation, we can describe the encoding and decoding functions, assuming the point x we are quantizing is in $\mathcal{V}_{q\Lambda}(0)$. We will also need an oracle $Q_\Lambda(x)$, which maps x to the closest point in Λ to x .

Algorithm 1 Encode

Input: $x \in \mathcal{V}_{q\Lambda}(0)$, Q_Λ
 $p \leftarrow Q_\Lambda(x)$
 $v \leftarrow G^{-1}p$ ▷ coordinates of p
return $v \bmod q$ ▷ quantized representation of p

Algorithm 2 Decode

Input: $c \in \mathbb{Z}_q^d$, Q_Λ
 $p \leftarrow Gc$ ▷ equivalent to answer modulo $q\Lambda$
return $p - qQ_\Lambda(\frac{p}{q})$

In practice, we will be using the Gosset (E_8) lattice as Λ with $d = 8$. This lattice is a union of D_8 and $D_8 + \frac{1}{2}$, where D_8 contains elements of \mathbb{Z}^8 with even sum of coordinates. There is a simple algorithm for finding the closest point in the Gosset lattice, first described in [25]. We provide the pseudocode for this algorithm together with the estimation of its runtime in Appendix B.

4.2 Matrix quantization

When quantizing a matrix, we normalize its rows, and quantize each block of d entries using the codebook. The algorithm 3 describes the quantization procedure for each row of the matrix.

Algorithm 3 NestQuant

Input: A — a vector of size $n = db, q$, array of β
 QA — n integers ▷ quantized representation
 B — b integers ▷ scaling coefficient indices
 $s \leftarrow \|A_i\|_2$ ▷ normalization coefficient
 $A \leftarrow \frac{A\sqrt{n}}{s}$
for $j = 0$ **to** $b - 1$ **do**
 $err = \infty$
 for $p = 1$ **to** k **do**
 $v \leftarrow A[dj + 1..dj + d]$
 $enc \leftarrow \text{Encode}\left(\frac{v}{\beta_p}\right)$
 $recon \leftarrow \text{Decode}(enc) \cdot \beta_p$
 if $err > |recon - v|_2^2$ **then**
 $err \leftarrow |recon - v|_2^2$
 $QA[dj + 1..dj + d] \leftarrow enc$
 $B_j \leftarrow p$
 end if
 end for
end for
Output: QA, B, s

We can take dot products of quantized vectors without complete dequantization using algorithm 4. We use it in the generation stage on linear layers and for querying the KV cache.

Algorithm 4 Dot product

Input: QA_1, B_1, s_1 and QA_2, B_2, s_2 — representations of two vectors of size $n = db$ from Algorithm 3, array β
 $ans \leftarrow 0$
for $j = 0$ **to** $b - 1$ **do**
 $p_1 \leftarrow \text{Decode}(QA_1[dj + 1..dj + d])$
 $p_2 \leftarrow \text{Decode}(QA_2[dj + 1..dj + d])$
 $ans \leftarrow ans + (p_1 \cdot p_2)\beta_{B_1[j]}\beta_{B_2[j]}$
end for
return ans

4.3 LLM quantization

Recall that we apply a rotation matrix H to every weight-activation pair of a linear layer without changing the output of the network. Let n be the number of input features to the layer.

- If $n = 2^k$, we set H to be Hadamard matrix obtained by Sylvester’s construction
- Otherwise, we decompose $n = 2^k m$, such that m is small and there exists a Hadamard matrix H_1 of size m . We construct Hadamard matrix H_2 of size 2^k using Sylvester’s construction, and set $U = H_1 \otimes H_2$.

Note that it’s possible to multiply an $r \times n$ matrix by H in $O(rn \log n)$ in the first case and $O(rn(\log n + m))$ in the second case, which is negligible to other computational costs and can be done online.

In NestQuant, we quantize all weights, activations, keys, and values using Algorithm 3. We merge the Hadamard rotation with the weights and quantize them. We also apply the Hadamard rotation and quantization to the activations before linear layers. We

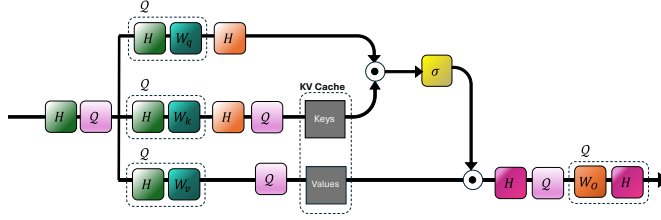


Figure 4: The quantization scheme of multi-head attention. H is Hadamard rotation described in 4.3. Q is the quantization function described in 4.2

also apply rotation to keys and queries, because it will not change the attention scores, and we quantize keys and values before putting them in the KV cache. Figure 4 illustrates the procedure for multi-head attention layers.

When quantizing a weight, we modify the NestQuant algorithm by introducing corrections to unquantized weights when a certain vector piece is quantized. We refer the reader to section 4.1 of [17] for a more detailed description.

4.4 Optimal scaling coefficients

One of the important parts of the algorithm is finding the optimal set of β_i . Given the distribution of 8-vectors that are quantized via a codebook, it is possible to find an optimal set of given size exactly using a dynamic programming approach, which is described in Appendix D.

4.5 Algorithm summary

Here we describe the main steps of NestQuant.

1. Collect the statistics for LDLQ. For each linear layer with in-dimension d , we compute a $d \times d$ matrix H .
2. We choose an initial set of scaling coefficients $\hat{\beta}$, and for each weight we simulate LDLQ quantization with these coefficients, getting a set of 8-dimensional vectors to quantize.
3. We run a dynamic programming algorithm described in Appendix D on the 8-vectors to find the optimal β -values for each weight matrix.
4. We also run the dynamic programming algorithm for activations, keys, and values for each layer. To get the distribution of 8-vectors, we run the model on a small set of examples.
5. We quantize the weights using LDLQ and precomputed β .
6. During inference, we quantize any activation before it's passed to the linear layer, and any KV cache entry before it is saved.

Note the complete lack of fine-tuning needed to make our method work.

5 Experiments

5.1 Simulated Data

We compared the mean L_2 loss per entry of SpinQuant to the uniform L_∞ -scaling quantizer (used in SpinQuant and other methods). The mean L_2 loss per entry for the product of two matrices $A \in \mathbb{R}^{n \times k}$, $B \in \mathbb{R}^{m \times k}$ is computed as $\frac{\|AB^T - \hat{A}\hat{B}^T\|_2}{nm}$. We set $n = k = m = 4096$ and sampled two matrices A, B with unit normal distribution $A_{ij}, B_{ij} \sim \mathcal{N}(0, 1)$. We compare to the lower bound from (1).

For NestQuant, we do a grid search over (q, k) . For given q and k , we find the best subset in $\{\frac{m}{2} \text{ for } m = 1, 2, \dots, 50\}$ of scaling coefficients β of size k using the algorithm from Appendix D. Then we calculate the expected bits per entry computed as $\log_2 q + \frac{1}{8} \sum_{i=1}^k p(\beta_i) \log_2 p(\beta_i)$ where $p(\beta_i)$ is the probability that the i 'th beta is used in quantization. In Figure 3, we plot the efficient frontier of bits per entry vs root mean L_2 loss.

q	Bits	Bits (no zstd)	W	W + KV	W + KV + A
14	3.99	4.06	6.308	6.379	6.633
12	3.76	3.83	6.376	6.475	6.841
10	3.50	3.57	6.486	6.640	7.251
8	3.18	3.25	6.700	6.968	7.989

Table 2: Wikitext2 perplexity of NestQuant quantization of Llama-3-8B at different rates. The "bits" column is the bit rate per entry with zstd compression of scaling coefficients, and "bits (no zstd)" is the bit rate without compression. The "W", "W+KV", and "W+KV+A" describe the quantization regime (whether weights, KV cache, or activations are quantized). The perplexity of non-quantized model is 6.139

5.2 Llama results

We quantize Llama-3-8B model [26] using different values of q . We choose the number of scaling coefficients (k) to be equal to 4, the Section 5.5 explains the rationale behind this choice. More details on the hyperparameter choice of the experiments are in Appendix E. For each experiment, we compute the number of bits per entry similar to Section 5.1, but for the setup of compressed β indices, we run the zstd compression algorithm instead of using the entropy of the distribution. As our evaluation metric, we use the perplexity on the validation split of wikitext2 with context length 2048.

We also perform the evaluation of NestQuant on various zero-shot benchmarks: ARC-Easy and ARC-Challenge [27], Hellaswag [28], [29], and Winogrande [30]. The results on 4-bit models with comparisons to other models are summarized in Table 1.

5.3 Comparison to other methods

We compare our method to the current state-of-the-art method *SpinQuant*. On the WikiText2 dataset, we computed the perplexity scores of the quantized models on context size 2048. Our method demonstrates superior perplexity scores by a high margin. On W4KV4A4 (4-bit weights, KV-cache, and activations) quantization of Llama 3-8B we achieve a perplexity score of 6.6 compared to the reported score of 7.3 in *SpinQuant* (See table 1). Impressively, our method outperforms *SpinQuant*, without the need of learned rotations. Even without LDLQ, we achieve a perplexity score of 6.8, which is still better than SpinQuant.

5.4 Results for other models

Here, we show the results of NestQuant on the newer 1B parameter model LLama3.2-1B. We do experiments in the same setups as for the Llama-3-8B model, computing the wikitext2 perplexity.

q	Bits	Bits (no zstd)	W	W + KV	W + KV + A
14	3.99	4.06	10.061	10.529	11.197
12	3.76	3.837	10.178	10.862	11.910
10	3.50	3.57	10.377	11.552	14.191
8	3.18	3.25	10.850	13.309	18.710

Table 3: Wikitext2 perplexity of NestQuant quantization of Llama-3.2-1B. The format of the table is the same as in Table 2. The perplexity of non-quantized model is 9.749

5.5 The choice of k

The value of k , i.e. the number of scaling coefficients is an important hyperparameter of the algorithm. With an increase of k , we decrease the quantization error by allowing each vector to be quantized to the lattice point with a proper scaling. However, it increases the bitrate and makes the encoding slower, since we need to try a larger number of scaling coefficients.

We used $k = 3, 4, 5, 8$ to quantize Llama-3-8B across different values of q , plotting the resulting perplexity against bitrate in Figure 5. We can see that using $k = 3$ leads to a suboptimal performance of the quantization scheme, while the performances of $k = 4, 5, 8$ are comparable. In our experiments, we use $k = 4$, because lower having k results in faster encoding.

More ablation studies for LDLQ and the choice of rotation are described in Appendix F.

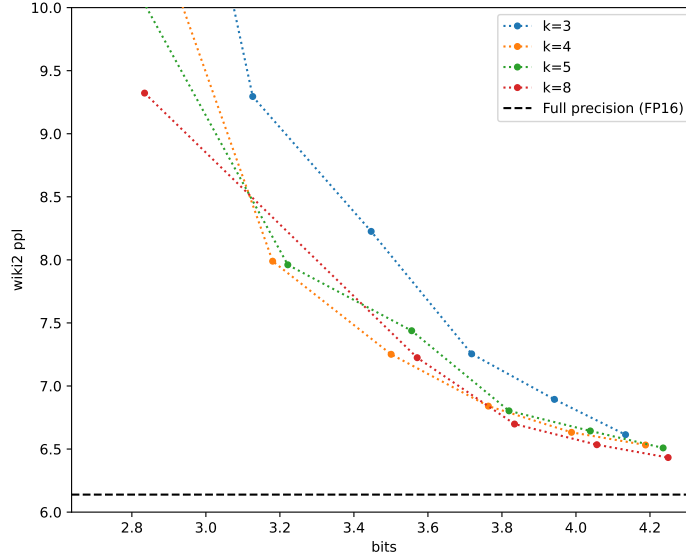


Figure 5: The perplexity-bitrate scaling of NestQuant with different values of k , all components of the model (weights, KV cache, activations) are quantized

6 Impact statement

This paper presents work whose goal is to advance the field of Machine Learning. There are many potential societal consequences of our work, none which we feel must be specifically highlighted here.

References

- [1] J. Conway and N. Sloane. A fast encoding method for lattice codes and quantizers. *IEEE Transactions on Information Theory*, 29(6):820–824, 1983.
- [2] Yury Polyanskiy and Yihong Wu. *Information theory: From coding to learning*. Cambridge university press, 2024.
- [3] Ram Zamir. *Lattice Coding for Signals and Networks: A Structured Coding Approach to Quantization, Modulation, and Multiuser Information Theory*. Cambridge University Press, 2014.
- [4] Adriaan J Stam. Limit theorems for uniform distributions on spheres in high-dimensional euclidean spaces. *Journal of Applied probability*, 19(1):221–228, 1982.
- [5] Allen Gersho. Asymptotically optimal block quantization. *IEEE Transactions on information theory*, 25(4):373–380, 1979.
- [6] Andy C Hung and Teresa H Meng. Multidimensional rotations for robust quantization of image data. *IEEE transactions on image processing*, 7(1):1–12, 1998.
- [7] Ran Hadad and Uri Erez. Dithered quantization via orthogonal transformations. *IEEE Transactions on Signal Processing*, 64(22):5887–5900, 2016.
- [8] Or Ordentlich and Yury Polyanskiy. Optimal quantization for matrix multiplication, 2024.
- [9] Moses S Charikar. Similarity estimation techniques from rounding algorithms. In *Proceedings of the thirty-fourth annual ACM symposium on Theory of computing*, pages 380–388, 2002.
- [10] Mayur Datar, Nicole Immorlica, Piotr Indyk, and Vahab S Mirrokni. Locality-sensitive hashing scheme based on p-stable distributions. In *Proceedings of the twentieth annual symposium on Computational geometry*, pages 253–262, 2004.
- [11] Alexandr Andoni and Piotr Indyk. Near-optimal hashing algorithms for approximate nearest neighbor in high dimensions. *Communications of the ACM*, 51(1):117–122, 2008.
- [12] Tim Dettmers, Mike Lewis, Younes Belkada, and Luke Zettlemoyer. Llm.int8(): 8-bit matrix multiplication for transformers at scale, 2022.

- [13] Guangxuan Xiao, Ji Lin, Mickael Seznec, Hao Wu, Julien Demouth, and Song Han. Smoothquant: Accurate and efficient post-training quantization for large language models, 2024.
- [14] Saleh Ashkboos, Amirkeivan Mohtashami, Maximilian L. Croci, Bo Li, Pashmina Cameron, Martin Jaggi, Dan Alistarh, Torsten Hoefler, and James Hensman. Quarot: Outlier-free 4-bit inference in rotated llms, 2024.
- [15] Zechun Liu, Changsheng Zhao, Igor Fedorov, Bilge Soran, Dhruv Choudhary, Raghuraman Krishnamoorthi, Vikas Chandra, Yuandong Tian, and Tijmen Blankevoort. Spinqant: Llm quantization with learned rotations, 2024.
- [16] Jun Li, Li Fuxin, and Sinisa Todorovic. Efficient riemannian optimization on the stiefel manifold via the cayley transform, 2020.
- [17] Albert Tseng, Jerry Chee, Qingyao Sun, Volodymyr Kuleshov, and Christopher De Sa. QuIP#: Even better llm quantization with hadamard incoherence and lattice codebooks, 2024.
- [18] Biing-Hwang Juang and Augustine H. Gray. Multiple stage vector quantization for speech coding. In *IEEE International Conference on Acoustics, Speech, and Signal Processing*, 1982.
- [19] Albert Tseng, Qingyao Sun, David Hou, and Christopher De Sa. Qtip: Quantization with trellises and incoherence processing, 2024.
- [20] Jerry Chee, Yaohui Cai, Volodymyr Kuleshov, and Christopher De Sa. Quip: 2-bit quantization of large language models with guarantees, 2024.
- [21] Elias Frantar, Saleh Ashkboos, Torsten Hoefler, and Dan Alistarh. Gptq: Accurate post-training quantization for generative pre-trained transformers, 2023.
- [22] Irit Dinur, Guy Kindler, Ran Raz, and Shmuel Safra. Approximating CVP to within almost-polynomial factors is np-hard. *Comb.*, 23(2):205–243, 2003.
- [23] Erik Agrell and Bruce Allen. On the best lattice quantizers. *IEEE Transactions on Information Theory*, 2023.
- [24] NVIDIA Corporation. nvcomp: Gpu-accelerated compression library, 2025. Accessed: 2025-01-30.
- [25] J. Conway and N. Sloane. Fast quantizing and decoding and algorithms for lattice quantizers and codes. *IEEE Transactions on Information Theory*, 28(2):227–232, 1982.
- [26] Llama Team, AI @ Meta. The llama 3 herd of models, 2024.
- [27] Peter Clark, Isaac Cowhey, Oren Etzioni, Tushar Khot, Ashish Sabharwal, Carissa Schoenick, and Oyvind Tafjord. Think you have solved question answering? try arc, the ai2 reasoning challenge, 2018.
- [28] Rowan Zellers, Ari Holtzman, Yonatan Bisk, Ali Farhadi, and Yejin Choi. Hellaswag: Can a machine really finish your sentence?, 2019.
- [29] Yonatan Bisk, Rowan Zellers, Ronan Le Bras, Jianfeng Gao, and Yejin Choi. Piqa: Reasoning about physical commonsense in natural language, 2019.
- [30] Keisuke Sakaguchi, Ronan Le Bras, Chandra Bhagavatula, and Yejin Choi. Winogrande: An adversarial winograd schema challenge at scale, 2019.
- [31] Stephen Merity, Caiming Xiong, James Bradbury, and Richard Socher. Pointer sentinel mixture models, 2016.

A Figures

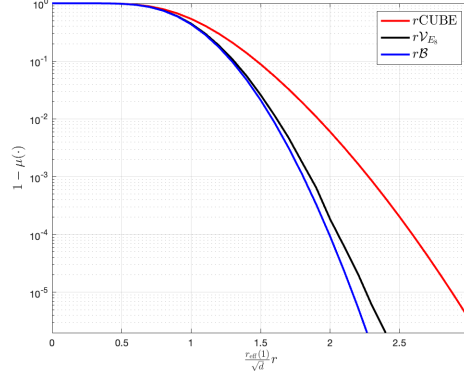


Figure 6: Complement Gaussian measure of a 8-dimensional cube (corresponding to shaping using an ℓ_∞ ball), a Voronoi region of the Gosset lattice E_8 (corresponding to shaping using Voronoi codes with base lattice E_8), and a Euclidean ball (corresponding to shaping with a ball, which does not admit efficient implementation)

B Gosset oracle

In this section, we discuss the algorithm for finding the nearest neighbour in E_8 lattice and estimate its performance in FLOPs (Floating Point Operations). We note that $E_8 = D_8 \cup D_8 + \frac{1}{2}$, where D_8 contains vectors in \mathbb{Z}_8 with even sum of coordinates. To compute $V_{E_8}(x)$, we compute two candidate points: $x_1 = V_{D_8}(x)$ and $x_2 = V_{D_8 + \frac{1}{2}}(x)$, and choose the one that has smaller L^2 distance to x .

To get $V_{D_8}(x)$, we can round each coordinate to the nearest integer. If the sum of rounded coordinates is odd, we need to "flip" the rounding direction of the coordinate for which the flip would cost the least. Note that finding the closest point in $V_{D_8 + \frac{1}{2}}$ works the same, but the rounding grid now contains half-integers, not integers.

In algorithm 5, we first round our vector down (getting d) and compute the mask (g) of whether it's optimal to round up for D_8 . We note that the optimal rounding for $D_8 + \frac{1}{2}$ is $d + 0.5$, while the optimal rounding for D_8 is $d + g$.

We want to understand whether rounding to D_8 or $D_8 + \frac{1}{2}$ is better. Let $dist_i$ be the absolute distance from the i -th entry $x_i \in [d_i, d_i + 1]$ to the middle of this integer segment $d_i + 0.5 = x_{2,i}$. We note that the contribution of this point to the MSE for D_8 is $(0.5 - dist_i)^2$, while for $D_8 + \frac{1}{2}$ is $dist_i^2$. The difference is: $0.25 - dist_i + dist_i^2 - dist_i^2 = 0.25 - dist_i$. If the sum of this value over i is negative (i.e. $\sum dist_i > 2$), it's optimal to quantize to D_8 , otherwise to $D_8 + \frac{1}{2}$. In pseudocode, we store $\sum dist_i$ as Δ

We note that we should check the constraint that the sum of coordinates in D_8 is even, and if it is not, "flip" one of the rounding directions. The optimal coordinate to flip can be determined through $dist$, and the new value of flipped coordinate — through g . We also need to update Δ given that the MSE difference changes.

The full pseudocode of the algorithm is in Algorithm 5.

Algorithm 5 Oracle for the Gosset lattice

```
1: Input:  $x \in \mathbb{R}^8$ 
2:  $d \leftarrow \text{floor}(x)$ 
3:  $x_2 \leftarrow d + 0.5$ 
4:  $g \leftarrow (x > x_2)$ 
5:  $s \leftarrow 2 \cdot g - 1$ 
6:  $x_1 \leftarrow d + g$ 
7:  $dist \leftarrow (x - x_2) \cdot s$ 
8:  $\Delta \leftarrow \sum_i dist_i$ 
9: if  $\sum_i x_{1,i}$  is odd then
10:    $pos = \text{argmin } dist$ 
11:    $x_{1,pos} \leftarrow x_{1,pos} - s_{1,pos}$ 
12:    $\Delta \leftarrow \Delta + 2 \cdot dist_{pos} - 1$ 
13: end if
14: if  $\sum_i x_{2,i}$  is odd then
15:    $pos = \text{argmax } dist$ 
16:    $x_{2,pos} \leftarrow x_{2,pos} + g_{2,pos}$ 
17:    $\Delta \leftarrow \Delta + 1 - 2 \cdot dist_{pos}$ 
18: end if
19: if  $\Delta > 2$  then
20:   return  $x_1$ 
21: else
22:   return  $x_2$ 
23: end if
```

C Crude estimate of runtime of quantized matrix

We give an estimate of how the NestQuant runtime affects the overall efficiency of the model. We note that the runtime of encoding and decoding one 8-vector with one scaled codebook is dominated by running the oracle for the Gosset lattice, described in Algorithm 5. By counting the arithmetic operations and comparisons equally, we get that one run of the oracle takes approximately 15 operations per vector entry. We should also add no more than 3 arithmetic operations in Algorithms 1 and 2, and multiplication by the generator matrix G , or its inverse G^{-1} . Given the structure of the matrices, we can spend less operations on multiplying them by vectors using prefix sum technique for G^{-1} and ignoring zeros for G . So, the multiplication takes around 2 operations per vector entry. In total, we do 20 FLOPs per dequantizing one matrix entry, and $20 \cdot k$ FLOPs for quantization, since we need to run the algorithm for k values of β . We note that in weight quantization the encoding time is not important since it's done offline, and in KV cache quantization encoding happens one time per token, while decoding happens with any additional query to the KV cache.

$$G^{-1} = \begin{pmatrix} 0.5 & 0.5 & 0.5 & 0.5 & 0.5 & 0.5 & 0.5 & -\frac{7}{2} \\ 0 & 1 & 1 & 1 & 1 & 1 & 1 & -\frac{6}{5} \\ 0 & 0 & 1 & 1 & 1 & 1 & 1 & -5 \\ 0 & 0 & 0 & 1 & 1 & 1 & 1 & -4 \\ 0 & 0 & 0 & 0 & 1 & 1 & 1 & -3 \\ 0 & 0 & 0 & 0 & 0 & 1 & 1 & -2 \\ 0 & 0 & 0 & 0 & 0 & 0 & 1 & -1 \\ 0 & 0 & 0 & 0 & 0 & 0 & 0 & 2 \end{pmatrix} \quad G = \begin{pmatrix} 2 & -1 & 0 & 0 & 0 & 0 & 0 & 0.5 \\ 0 & 1 & -1 & 0 & 0 & 0 & 0 & 0.5 \\ 0 & 0 & 1 & -1 & 0 & 0 & 0 & 0.5 \\ 0 & 0 & 0 & 1 & -1 & 0 & 0 & 0.5 \\ 0 & 0 & 0 & 0 & 1 & -1 & 0 & 0.5 \\ 0 & 0 & 0 & 0 & 0 & 1 & -1 & 0.5 \\ 0 & 0 & 0 & 0 & 0 & 0 & 1 & 0.5 \\ 0 & 0 & 0 & 0 & 0 & 0 & 0 & 0.5 \end{pmatrix} \quad (4)$$

Recall that in generation phase the LLM runtime is memory-bound, i.e. getting the weights from memory takes significantly more time than computing the matrix-vector product. Let's compute the total running time of loading matrix of size $m \times n$ from memory, which can be decomposed into the following running times:

1. Loading the matrix from memory $mnRT_{\text{load}}/8$ seconds, where R is the rate (bits/entry) and T_{load} is the time to load a byte (in seconds)
2. Decoding the matrix $N_{\text{decode}} \cdot mn \cdot T_{\text{flop}}$ where N_{decode} is the number of operations per entry and T_{flop} is the time to apply a floating point operation to a byte.

In total $T_{\text{total}} = mn(RT_{\text{load}}/8 + T_{\text{flop}}N_{\text{decode}})$ compared to $mn \cdot 2T_{\text{load}}$ (assume 16-bit baseline), so the speedup is $\frac{2T_{\text{load}}}{RT_{\text{load}}/8 + T_{\text{flop}}N_{\text{decode}}}$.

Defining the arithmetic intensity $\alpha = \frac{T_{\text{load}}}{T_{\text{flop}}}$, we get a theoretical speedup of $\frac{2\alpha}{R\alpha/8+N_{\text{decode}}}$. In our implementation of quantization $N_{\text{decode}} = 20$ and $\alpha \approx 30$, For $R = 4$ we should expect a theoretical speedup of $\frac{60}{35} \approx 1.71$. For $R = 3$ we get a theoretical speedup of $\frac{62}{33.25} \approx 1.92$.

In summary, we expect NestQuant in to achieve speedup in two following ways:

- By speeding up the retrieval of weights and KV cache entries
- By quantizing activations for large models, where weights are stored on different GPUs, and there are bandwidth limitations.

D Dynamic programming for optimal β

Recall that instead of using one instance of lattice codebook C , we use a union of codebooks C scaled to different coefficients. Specifically, our final codebook \mathcal{C} is parameterized by coefficients $\beta_1 \leq \beta_2 \leq \dots \leq \beta_k$, and is equal to:

$$\mathcal{C} = \beta_1 C \cup \beta_2 C \cup \dots \cup \beta_k C$$

Given a set of 8-vectors to quantize, we can find the set of β that minimizes reconstruction error using a dynamic programming algorithm, which is described in Appendix D.

When quantizing a vector to the i -th scaled codebook, we could either get a small granular error when the vector is in $V_{\beta_i \Lambda}(0)$, or a large overload error otherwise. If we use a codebook with smaller β , we have larger chance of overload error, but the expected magnitude of granular error is smaller due to the volume of Voronoi region being smaller (Figure 7). We can have two strategies for encoding:

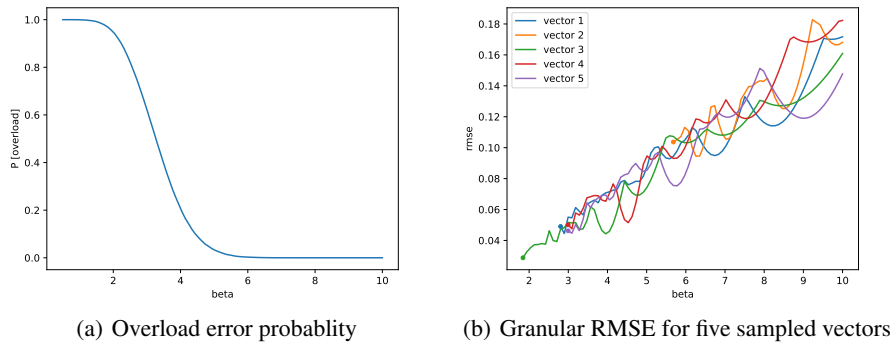


Figure 7: Granular and overload error for standard Gaussian vectors, $q = 16$

1. **First- β** : Use the smallest β , which does not result in an overflow error.
2. **Opt- β** : Try all the values of β , and choose the one that has the smallest reconstruction MSE.

K	2	4	6	8	10
OPT- β	0.0878	0.0795	0.0708	0.0669	0.0646
FIRST- β	0.0878	0.0798	0.0712	0.0676	0.0656

Table 4: Mean RMSE for reconstructed iid standard Gaussian 8-vectors, $q = 16$, k betas are uniform on $[0, 10]$.

Even though Opt- β should provide smaller error, the definition of First- β will be useful for us. We can note that the difference between error for Opt- β and First- β is not very significant (Table D). Moreover, First- β can be used to determine the optimal set of β_i to use.

Let we have n samples v_1, v_2, \dots, v_n from the distribution of vectors we are quantizing, and a large set of betas B , containing $\beta_1 < \beta_2 < \dots < \beta_m$, from which we want to take the optimal subset of size k which minimizes the loss under First- β strategy. For each vector v_i and beta β_j we compute mse_{ij} — the MSE if we use β_j to quantize v_i and $overload_{ij}$ — whether an overload error occurs in this scenario.

We solve the optimization problem with dynamic programming. Let’s define dp_{ij} be the minimum sum of MSE we can get if we have to quantize all the vectors which do not yield an overload error for β_i , using β_i and $j - 1$ smaller betas and First- β strategy. If i is large enough so that no vector has an overflow error on β_i , dp_{ik} has the answer to the problem. To compute the value of dp_{ij} , we can iterate over s — the index of second largest beta in the set (the largest being β_i). Then, the recalculation works in the following way:

$$dp_{ij} \leftarrow \min \left(dp_{ij}, dp_{s,j-1} + \sum_{p, cond_p} mse_{pi} \right)$$

where $cond_p = overload_{ps} \wedge \neg overload_{pi}$

By following the transtions in this dynamic programming, we can reconstruct the optimal set of β .

Algorithm 6 Dynamic programming for finding the set of β

```

1: Input: vectors  $v_i$ , beta set  $B$ ,  $mse_{ij}$ ,  $overload_{ij}$ 
2:  $dp_{i,j} = \infty$  for  $i$  in  $0 \dots m$ ,  $j$  in  $0 \dots k$ 
3:  $from_{i,j} = \text{null}$  for  $i$  in  $0 \dots m$ ,  $j$  in  $0 \dots k$ 
4:  $dp_{0,0} = 0$ 
5: for  $i = 1$  to  $m$  do
6:   for  $j = 1$  to  $k$  do
7:     for  $s = 0$  to  $i - 1$  do
8:        $cond_p = overload_{ps} \wedge \neg overload_{pi}$  for  $p \in 1 \dots n$ 
9:        $cost = \sum_p cond_p \cdot mse_{pi}$ 
10:      if  $dp_{ij} > dp_{s,j-1} + cost$  then
11:         $dp_{ij} \leftarrow dp_{s,j-1} + cost$ 
12:         $from_{ij} \leftarrow s$ 
13:      end if
14:    end for
15:  end for
16: end for
17: Let  $pos$  is chosen so that  $\beta_{pos}$  has no overflow errors
18: result = []
19: for  $j = k$  downto 1 do
20:   result.append( $pos$ )
21:    $pos \leftarrow from_{pos,j}$ 
22: end for

```

E Llama experiment details

We choose the train split of the Wikitext2 [31] dataset as a calibration dataset for computing H , and evaluate the model on the validation split, computing the perplexity metric. For step 2 in the algorithm (Section 4.5), we select $\hat{\beta} = [3.5, 4.5, 6.0, 14.5, 25.0]/q$, because it is the β we get when optimizing them for weight quantization without consideration of LDLQ. The overall universe of betas contains values from 1 to 40 with spacing ranging from 0.25 to 2. For running DP on activations, keys, and values, we run the model on a batch of 6 full-length sequences, which is sufficient for this low-dimensional hyperparameter.

When choosing maximum beta for given distribution, we add a margin of $\frac{3.0}{q}$ for weights and $\frac{4.0}{q}$ to the maximum beta needed to have 0 overload errors on known data to account for potential overload errors in unknown data. While small number of overload error does not affect prplxity significantly, we still aim to minimize their probability.

When computing perplexity for Wikitext2 with given context length, we average the perplexities for all the positions, which is standard for other works in quantization of LLMs.

F Ablation studies

We found LDLQ to be useful in improving the quality of quantized model. In table 5, we compare the wikitext2 perplexity of models with and without LDLQ.

Algorithm	W	W + KV	W + KV + A
NestQuant	6.308	6.379	6.633
NestQuant (no LDLQ)	6.528	6.605	6.849

Table 5: Effect of LDLQ on NestQuant ($q = 14$ and $k = 4$) wikitext2 perplexity

While Hadamard matrices from Sylvester construction are commonly used in other works (QuIP#, Quarot), there are multiple ways to construct a fast rotation for the case when dimension is not a power of 2 (such as the down projection in MLP of Llama-3). We tested three possible options for rotation on $q = 14$, $k = 4$, W + KV + A quantization.

Algorithm	W + KV + A
Fourier	6.773
$S \otimes H$, S — orthogonal, H — Sylvester Hadamard	6.770
$H_1 \otimes H$, H_1 — hardcoded Hadamard, H — Sylvester Hadamard	6.663

Table 6: Effect of rotation on NestQuant ($q = 14$ and $k = 4$) wikitext2 perplexity